HHS Public Access

Author manuscript

Neuroscience. Author manuscript; available in PMC 2020 March 15.

Published in final edited form as:

Neuroscience. 2019 March 15; 402: 51–65. doi:10.1016/j.neuroscience.2019.01.012.

Role of $Na_V1.6$ and $Na_V\beta4$ sodium channel subunits in a rat model of low back pain induced by compression of the dorsal root ganglia

Wenrui Xie, **Jingdong Zhang**, **Judith A. Strong**, and **Jun-Ming Zhang**

Pain Research Center, Department of Anesthesiology, University of Cincinnati College of Medicine, 231 Albert Sabin Way, ML0531, Cincinnati, OH, 45267-0531, USA

Abstract

Low back pain is a common cause of chronic pain and disability. It is modeled in rodents by chronically compressing the lumbar dorsal root ganglia (DRG) with small metal rods, resulting in ipsilateral mechanical and cold hypersensitivity, and hyperexcitability of sensory neurons. Sodium channels are implicated in this hyperexcitability, but the responsible isoforms are unknown. In this study, we used siRNA- mediated knockdown of the pore-forming $Na_V1.6$ and regulatory $Na_V\beta4$ sodium channel isoforms that have been previously implicated in a different model of low back pain caused by locally inflaming the L5 DRG. Knockdown of either subunit markedly reduced spontaneous pain and mechanical and cold hypersensitivity induced by DRG compression, and reduced spontaneous activity and hyperexcitability of sensory neurons with action potentials <1.5 msec (predominately cells with myelinated axons, based on conduction velocities measured in a subset of cells) 4 days after DRG compression. These results were similar to those previously obtained in the DRG inflammation model and some neuropathic pain models, in which sensory neurons other than nociceptors seem to play key roles. The cytokine profiles induced by DRG compression and DRG inflammation were also very similar, with upregulation of several type 1 pro-inflammatory cytokines and downregulation of type 2 anti-inflammatory cytokines. Surprisingly, the cytokine profile was largely unaffected by $Na_V\beta4$ knockdown in either model. The $Na_V1.6$ channel, and the $Na_V\beta4$ subunit that can regulate $Na_V1.6$ to enhance repetitive firing, play key roles in both models of low back pain; targeting the abnormal spontaneous activity they generate may have therapeutic value.

Keywords

Radicular pain; spontaneous activity; cytokine; sympathetic nervous system; sensory neuron; inflammation

Corresponding author: Jun-Ming Zhang, M.D., M.Sc. at above address, Phone: 513-558-2427, Fax: 513-558-0995, Jun-Ming.Zhang@uc.edu.

Introduction:

Chronic low back pain is a major cause of disability and driver of health care costs. For many patients, current treatment methods are not effective (Institute of Medicine (US) Committee on Advancing Pain Research C, and Education., 2011). A number of preclinical models of low back pain have been developed. These share some common features, including hyperexcitability and abnormal spontaneous activity of primary sensory neurons in the lumbar dorsal root ganglia (DRG) that is partly dependent on upregulation of sodium channels (Strong JA et al., 2013). DRG express multiple isoforms of voltage-gated sodium channel pore-forming α subunits and regulatory β subunits. Many studies of pain mechanisms have focused on the α subunit $Na_V1.7$, because its loss in humans leads to congenital insensitivity to pain, and because it is expressed in nociceptors but few other excitable tissues (Barbosa C and Cummins TR, 2016;Dib-Hajj SD et al., 2010). However, studies in a model of low back pain induced by local inflammation of the lumbar DRG (LID model) showed that the α (pore-forming) subunit $Na_V1.6$ played a key role; siRNA-mediated knockdown of the channel largely blocked development of pain behaviors and abnormal sensory neuron hyperexcitability and spontaneous activity (Xie W et al., 2013). This isoform (gene name, Scn8a) is found throughout the brain and is also in the heart, so it has received less attention as a possible therapeutic target. Very similar results were obtained in the LID model by knocking down the regulatory β subunit $Na_V\beta4$ (Xie W et al., 2016), an effect proposed to depend on both the subunit's ability to increase repetitive firing and hyperexcitability by increasing persistent and resurgent currents through $Na_V1.6$ channels, and on its ability to regulate expression of $Na_V1.6$ (Barbosa C and Cummins TR, 2016;Raman IM and Bean BP, 1997).

Another model of low back pain, the chronic compression of the DRG (CCD) model, involves compressing the L4/L5 DRGs in rat (or corresponding DRGs in mice) with small metal rods inserted into the foramen in rats or mice (Fan N et al., 2011;Hu SJ and Xing JL, 1998;Song XJ et al., 1999). This was developed in order to model certain types of low back pain in which the DRG is compressed, for example by stenosis or laterally herniated discs. Previous studies have shown that, like the DRG inflammation model, the CCD model results in hyperexcitability and spontaneous activity of sensory neurons in the compressed DRG (Hu SJ and Xing JL, 1998;Ma C et al., 2006;Song Y et al., 2012;Zhang J-M et al., 1997). Several studies support a role of sodium channels in these electrophysiological changes, including roles for the persistent sodium current and both tetrodotoxin (TTX)-sensitive and TTX-resistant sodium currents(Fan N et al., 2011;Fan N,Sikand P,Donnelly DF,Ma C and Lamotte RH, 2011;Song XS et al., 2009;Song Y,Li HM,Xie RG,Yue ZF,Song XJ,Hu SJ and Xing JL, 2012;Tan ZY et al., 2006). However, to our knowledge, few studies have examined which sodium channel isoforms might mediate these electrophysiological changes.

Another feature common to many preclinical low back pain models is the importance of localized inflammation around the DRG(Strong JA,Xie W,Bataille FJ and Zhang JM, 2013). In the LID model, this aspect is modeled directly by injecting the immune stimulator zymosan over the L5 DRG in rats(Xie WR et al., 2006). The CCD model, despite having a very different type of immune stimulus, has also been shown to cause localized inflammation in the DRG, including satellite glia activation (Zhang H et al., 2009) and

upregulation of several pro-inflammatory cytokines(White FA et al., 2005;Yu Y et al., 2017). Reduction in pain behaviors by anti-inflammatory drugs has also been demonstrated (Gu X et al., 2007;Gu X et al., 2007;Han WJ et al., 2015;Huang ZJ et al., 2011;Ma ZL et al., 2007;Nahm FS et al., 2017;Watanabe K et al., 2011). Sensory neurons are one source of cytokines, express cytokine receptors, and respond to cytokines with changes in excitability (White FA, Sun J, Waters SM, Ma C, Ren D, Ripsch M, Steflik J, Cortright DN, Lamotte RH and Miller RJ, 2005;Yu Y, Huang X, Di Y, Qu L and Fan N, 2017). The CCD model may also make sensory neurons more sensitive to inflammatory mediators in addition to increasing other measures of excitability (Ma C, Greenquist KW and Lamotte RH, 2006;White FA, Sun J, Waters SM, Ma C, Ren D, Ripsch M, Steflik J, Cortright DN, Lamotte RH and Miller RJ, 2005;Zhang J-M, Song XJ and LaMotte RH, 1997).

The objective of the present study was to determine whether the $Na_V1.6$ and $Na_V\beta4$ channel isoforms that play a key role in the LID model might also play a role in the CCD model, despite it having very different immunological stimulus. In addition, we conducted a more extensive profiling of the cytokines regulated by the CCD model, and examined for the first time whether Na channel knockdown regulates cytokines in these back pain models.

Methods:

Animals:

The experimental protocol was approved by the Institutional Animal Care and Use Committee of the University of Cincinnati. Experiments were conducted in accordance with the National Institutes of Health Guide for the Care and Use of Laboratory Animals. Sprague Dawley rats of both sexes (Envigo, Indianapolis, USA) weighing 200–250 g at the time of pain model surgery were used in approximately equal numbers, unless otherwise indicated. Rats were housed two per cage at 22 ± 0.5°C under a controlled diurnal cycle of 14-h light and 10-h dark.

Surgical procedures for pain models, microsympathectomy, and siRNA injections

The CCD model was implemented as previously described (Song XJ, Hu SJ, Greenquist KW, Zhang JM and LaMotte RH, 1999;Zhang J-M et al., 1999). Briefly, rats were anesthetized with isoflurane. The skin above the spine was cut at the midline from L6-L3. On the right side, the paraspinal muscles were separated along the spine and the transverse process and intervertebral foramina of L4 and L5 were exposed. A 25 G needle bent at a right angle was inserted approximately 2 mm into the intervertebral foramen at L4 and L5, at an angle of 30–40 degree toward head. Then the needle was withdrawn followed by implanting a stainless L-shaped steel rod, 3 mm in length and 0.63 mm in diameter into each foramen, at L4 and L5 ganglion following the path as described for the needle. After rods were implanted, the wound was closed by suturing muscle and skin layers. In some experiments, just prior to the insertion of the metal rods, siRNA was injected into both DRGs through a small glass needle (75 μm o.d.) inserted close to the DRG through a small hole cut into the overlying membrane close to the site where the dorsal ramus exits the spinal nerve, as previously described (Xie W et al., 2012). siRNAs directed against rat $Na_V\beta4$ subunit (Scn4b; gene ID 315611), rat $Na_V1.6$ (Scn8a, gene ID 29710) or firefly

luciferase (nontargeting control) were designed by and purchased from Dharmacon/ThermoFisher (Lafayette, CO). The $Na_V\beta4$-siRNA and $Na_V1.6$ siRNAs were each siGENOME™ siRNA consisting of a "smartpool" of four different siRNA constructs combined into one reagent. Catalog numbers were M-101002–01 (directed against $Na_V\beta4$), M-094591–00 (directed against $Na_V1.6$) and D-001210–02 (nontargeting control directed against firefly luciferase, screened to have minimal off-target effects and least 4 mismatches with all known human, mouse and rat genes according to the manufacturer). The luciferase sequence (UAAGGCUAUGAAGAGAUAC) is unrelated to the shRNA sequence recently reported to have extensive off-target effects in hippocampal neurons (Hasegawa Y et al., 2017). Sequences for the 2 sodium channel constructs may be obtained from our previous publications (Xie W, Strong JA, Ye L, Mao JX and Zhang J-M, 2013;Xie W, Tan ZY, Barbosa C, Strong JA, Cummins TR and Zhang J-M, 2016), which also describe the extensive validation of these two siRNAs. We previously found electrophysiological properties of normal DRGs injected with the control siRNA used were very similar to those in naïve DRGs (Xie W, Strong JA, Ye L, Mao JX and Zhang J-M, 2013).

The local inflammation of the DRG model (LID) was implemented as previously described (Xie W et al., 2012). Briefly, the DRGs were exposed as described above, then inflamed by depositing the immune activator zymosan (2 mg/ml, 10 μl, in incomplete Freund's adjuvant) over the DRG as previously described; both the L4 and L5 DRGs were inflamed in order to increase the amount of protein available for cytokine measurements and to match the CCD experiments.

"Microsympathectomy" (mSYMPX) was performed as previously described (Xie W et al., 2016), 6 days prior to the CCD surgery. Briefly, the L4 and L5 spinal nerves and transverse processes were exposed. The spinal nerves (ventral rami) were visualized and freed from surrounding tissue. The gray rami enter the L4 and L5 spinal nerves close to the DRGs (i.e. coming from the L3 and L4 sympathetic paravertebral ganglia according to the nomenclature of Baron (Baron R et al., 1988)), near the site at which the gray ramus merges into the spinal nerve. Here, the gray rami and nearby connective tissue were gently dissected away from the nearby blood vessels and cut and disconnected from the spinal nerve. Around 1 mm of gray ramus was further removed to make a gap and slow regeneration. Sham controls received similar exposure of the spinal nerves but the gray rami were not cut.

Immunohistochemistry

DRG sections were cut at 40 μm on a cryostat after fixation in 4% paraformaldehyde in 0.1M Phosphate Buffer and 4% sucrose. The rabbit polyclonal antibody against $Na_V1.6$ was from Alomone (Jerusalem, Israel; catalog ASC-009) used at 1:150 dilution. The antibody specificity was previously demonstrated by a lack of staining in a knockout mouse (Black JA et al., 2002) and by observing knockdown of the signal in rat DRG with siRNA methods, including knockdown by several individual siRNA constructs with distinct sequences (Xie W et al., 2015). The rabbit polyclonal antibody against $Na_V\beta4$ antibody was from Alomone (catalog ASC-044) used at a dilution of 1:150. This antibody has been previously validated by observing knockdown of the signal in rat DRG with siRNA using immunohistochemical and Western blot methods, including knockdown by several individual siRNA constructs

with distinct sequences (Xie W, Tan ZY, Barbosa C, Strong JA, Cummins TR and Zhang J-M, 2016). The secondary antibody conjugated to Alexa Fluor 594 (Invitrogen, Carlsbad, CA) was used at a dilution of 1:1000. Images from multiple sections of each DRG were captured under an Olympus BX61 fluorescent microscope using Slidebook 4.1 imaging acquisition software (Intelligent Imaging Innovation, Denver, CO). To measure the expression of $Na_V1.6$ or $Na_V\beta4$ in the DRG neurons, the summed intensities of the signal were measured and normalized by the cellular area in each analyzed section to give an intensity ratio. Intensity measurements were always conducted in a side-by-side design, with sections from control and CCD DRG analyzed under the same conditions. Data are presented with intensities in CCD DRG normalized to the paired control DRG. In other experiments, $Na_V1.6$ or $Na_V\beta4$ was costained with the neuronal marker NeuN using a mouse monoclonal antibody (Abcam, catalog# ab104224 at dilution 1:200 and secondary antibody Goat anti-mouse IgG (Alexa Fluor 488) at dilution 1:1000). In each section all NeuN positive neurons were outlined and scored as Na-channel positive or negative, in order to examine the cell size distributions. For the data plots, the measured areas of each cell were converted to effective diameters based on a circle having the same area.

Multiplex Cytokine Measurement

Protein was isolated from inflamed or compressed DRGs, or DRGs taken from sham-operated controls, 4 days after siRNA injection and implementation of the pain model. The same sham group was compared to both inflamed and compressed DRG models; this sham surgery consisted of exposing the L4 and L5 DRG as similarly done for both pain models. Cytokine expression profiles were examined using a Bio-Plex System (Bio-Rad, Hercules, CA, USA) combined with Millipore Rat Cytokine/Chemokine Magnetic Bead Panel (catalog number RECYMAG65K27PMX, EMD Millipore, Billerica, MA, USA, selected subset of available analytes). A total of 20 rat cytokines was measured simultaneously from a single well according to the manufacturer's protocols and as in our previous studies (Xie W, Chen S, Strong JA, Li A-L, Lewkowich IP and Zhang J-M, 2016;Xie WR, Deng H, Li H, Bowen TL, Strong JA and Zhang J-M, 2006). Full names, systemic names, and alternative names of the cytokines examined are given in Table 1.

Pain behavior measurements

Behavioral data presented are all from the ipsilateral side; as in the original description of the CCD model used (Song XJ, Hu SJ, Greenquist KW, Zhang JM and LaMotte RH, 1999) the contralateral behaviors showed no or relatively small changes from baseline (data not shown). Mechanical sensitivity was tested by applying a series of von Frey filaments to the heel region of the paws, using the up-and-down method (Chaplan SR et al., 1994). A cutoff value of 15 grams was assigned to animals that did not respond to the highest filament strength used. A wisp of cotton pulled up from, but still attached to a cotton swab was stroked mediolaterally across the plantar surface of the hindpaws to score the presence or absence of a brisk withdrawal response to a normally innocuous mechanical stimulus (light touch-evoked tactile allodynia). This stimulus does not evoke a response in normal animals. Cold sensitivity was scored as withdrawal responses to a drop of acetone applied to the ventral surface of the hind paw. When observed, responses to acetone or light brush strokes consisted of several rapid flicks of the paw and/or licking and shaking of the paw; walking

movements were not scored as positive responses. Spontaneous guarding behavior was scored (Xu J and Brennan TJ, 2010) as 0 (no guarding, paw flat on floor), 1 (mild shift of weight away from paw), 2 (unequal weight bearing and some part of the foot not touching the floor), or 3 (foot totally raised or not bearing any weight); these scores were recorded just before each application of the von Frey filament (6 observations per paw total) and averaged.

Electrophysiology

Intracellular recording in current clamp mode was performed at 36 – 37°C with an Axoclamp 2B using sharp microelectrodes on sensory neurons near the dorsal surface of an acutely isolated whole DRG preparation, as previously described (Xie W, Strong JA, Kim D, Shahrestani S and Zhang JM, 2012). This preparation allows neurons to be recorded without enzymatic dissociation, with the surrounding satellite glia cells and neighboring neurons intact (Song XJ, Hu SJ, Greenquist KW, Zhang JM and LaMotte RH, 1999;Zhang J-M, Song XJ and LaMotte RH, 1999). The DRG was perfused with artificial cerebrospinal fluid (in mM: NaCl 130, KCl 3.5, NaH_2PO_4 1.25, $NaHCO_3$ 24, Dextrose 10, $MgCl_2$ 1.2, $CaCl_2$ 1.2, 16 mM HEPES, pH = 7.3, bubbled with 95% O_2/ 5% CO_2). Excitability parameters were analyzed as described previously (Xie W, Strong JA and Zhang JM, 2015). Briefly, after measurement of any stable spontaneous activity, action potential parameters were measured during the smallest depolarizing current that could evoke an action potential (rheobase). For cells with spontaneous activity, the resting potential was taken as an average value observed between action potentials. Longer (270 msec) suprathreshold current steps were then applied to determine the maximum number of action potentials that could be evoked, and whether subthreshold membrane oscillations (with characteristic frequencies in the range of 100 – 200 Hz) could be evoked. Presence or absence of these distinctive subthreshold oscillations was determined by visual inspection of the traces. All the electrophysiological data was analyzed by a single experimenter. For the data presented, cells were classified into two groups based on the action potential duration being less than or greater than 1.5 msec, putatively corresponding to cells with myelinated and unmyelinated axons, respectively (see Results). A subset of cells in which axon conduction velocity could be measured (stimulation of attached dorsal root) were classified as follows: <1.2 m/s, C; or myelinated: >= 7.5 m/s, Aβ; between 1.2 and 7.5 m/s, Aδ (Stebbing MJ et al., 1999). As in our previous studies there were few Aδ cells (5 – 9% of cells with measured conduction velocity, in the 4 experimental groups) and the properties of the cells with myelinated axons were dominated by the Aβ cells. In this study we used larger animals for electrophysiology than used in our previous studies, in order to have the degree of DRG compression be similar to that obtained in behavioral and biochemical studies; the larger/older DRG preparations had a lower percentage of cells (49.8%) in which a conduction velocity could be obtained than in some of our previous studies.

Statistics and data analysis

Two-sided statistical tests were used throughout. Data was analyzed using Graphpad Prism, Version 6. Behavioral time course data were analyzed using two-way repeated measures ANOVA with Holm-Sidak's post hoc test to determine on which days $Na_V1.6$ and $Na_V\beta4$ knockdown groups differed from the control siRNA group, or to determine when the

sympathectomized group differed from the sham sympathectomized group. For cytokine data, fold changes in concentrations of cytokine (i.e. normalized to the sham group) were analyzed using log-transformed values. Cytokine data were analyzed within each pain model group (i.e., CCD or LID); the sham group (no pain model), pain model + control siRNA group, and pain model plus Na_VB4 knockdown group were analyzed using one-way ANOVA followed by Tukey's posttest comparing each group to every other group. For immunohistochemical quantification of sodium channel expression, values obtained from multiple images from each rat were averaged, and the statistical analysis was conducted on these averages using the number of rats as the N value for each group. For continuous electrophysiological data, comparison of values between different experimental groups was done using the Kruskal-Wallis test with Dunn's posttest to examine the effect of CCD (CCD + control siRNA group vs. normal) and the effect of sodium channel knockdown (CCD + control siRNA group vs. CCD + $Na_V1.6$ and $Na_V\beta4$ knockdown groups). The nonparametric method was chosen because most of the electrophysiological data did not show a normal distribution based on the D'Agostino and Pearson omnibus normality test. The statistical test used in each case is indicated in the text, or figure legend. Significance was ascribed for $p<0.05$. Levels of significance are indicated by the number of symbols, e.g., *, $p = 0.01$ to <0.05; **, $p = 0.001$ to 0.01; ***, $p < 0.001$. Data are presented as average ± S.E.M.

Results:

CCD causes upregulation of $Na_V1.6$ but not $Na_V\beta4$

Sample images of $Na_V1.6$ immunohistochemical staining in DRG sections from normal DRG, and from compressed DRGs on day 4, are shown in figure 1. As previously reported, $Na_V1.6$ was expressed in a wide range of neuron sizes, with somewhat higher representation in cells in the middle range of diameters, both before and 4 days after CCD (figure 2A, B). The overall intensity of $Na_V1.6$ immunoreactivity increased in both the L4 and L5 DRGs; the overall average increase was 1.8 ± 0.26 -fold after CCD (Figure 2C). This was primarily due to increased intensity within labeled cells, as the percentage of $Na_V1.6$-positive cells increased only slightly (from 35% to 39%).

Examples of immunohistochemical staining of $Na_V\beta4$ are shown in Figure 3. As previously observed, it was expressed in a subset of neurons, with the size distribution skewed away from the smallest neurons, both before and 4 days after CCD (Figure 4). The overall intensity of $Na_V\beta4$ immunoreactivity was not significantly affected by CCD (average ratio of CCD/normal was 0.91 ± 0.06, not significantly different from 1). The percentage of $Na_V\beta4$-positive neurons increased slightly from 30% in normal rats to 36% in CCD rats.

Knockdown of $Na_V1.6$ or $Na_V\beta4$ reduces pain behaviors in the CCD model.

To determine the effects of sodium channel knockdown on pain behaviors induced by DRG compression, the L4 and L5 DRGs were injected with siRNA directed against $Na_V1.6$ just prior to DRG compression. Control animals received injection of a non-targeting control siRNA. In a separate experiment, experimental groups received siRNA directed against $Na_V\beta4$ or the control siRNA. The control groups in these two experiments were very similar, and the effects of $Na_V\beta4$ and $Na_V1.6$ knockdown were also very similar. Both experiments

are presented and analyzed together in Figure 5, with the two control groups combined into a single group. Data from both sexes were combined; no obvious sex differences were observed though the study was not powered to examine this in detail. As shown in figure 5, knockdown of either sodium channel subunit markedly reduced static and dynamic mechanical allodynia for the duration of the experiment (4 weeks). Reduction of cold allodynia and guarding behavior (a measure of spontaneous pain) were also highly significant overall, though not reaching significance on every experimental day in the posttests.

Microsympathectomy reduces pain behaviors in the CCD model

Because the behavioral effects of $Na_V1.6$ or $Na_V\beta4$ knockdown appeared very similar to the results previously obtained in the DRG inflammation model, we examined whether pain behaviors in the CCD model could be ameliorated by prior “microsympathectomy”, as previously shown for the DRG inflammation model (Xie W, Chen S, Strong JA, Li A-L, Lewkowich IP and Zhang J-M, 2016). The microsympathectomy, i.e., cutting of the grey rami near the L4 and L5 DRG, was conducted 6 days prior to DRG compression. Control animals received a sham surgery, exposing the grey rami but not cutting them. As shown in figure 6, the microsympathectomy had no effect on baseline behaviors but strongly reduced static and dynamic mechanical responses and cold allodynia after DRG compression.

Knockdown of $Na_V1.6$ or $Na_V\beta4$ reduces CCD-induced hyperexcitability of sensory neurons with narrow action potentials

DRG compression has previously been shown to result in hyperexcitability and spontaneous activity of sensory neurons in the compressed DRGs (see Introduction). In order to determine whether $Na_V1.6$ and $Na_V\beta4$ played a role in this hyperexcitability, siRNA-mediated knockdown of these channels was conducted using the same protocol as used for the behavior experiments shown in Figure 5: Non-targeting or Na-channel specific siRNA was injected at the time of DRG compression, and DRG were isolated 4 days later for microelectrode recording in a whole DRG preparation. Recordings from normal DRG (no pain model) were also conducted.

In cells with action potential durations <1.5 msec, DRG compression resulted in a marked increase in spontaneous activity, decrease in rheobase, resting membrane depolarization, increase in percentage of cells in which multiple action potentials could be elicited by suprathreshold current injection, and increase in the incidence of subthreshold membrane oscillations during spontaneous activity or current injection, almost all of which were largely ameliorated by knockdown of either $Na_V1.6$ or $Na_V\beta4$ (Figure 7). The spontaneous activity observed in the CCD/control siRNA group consisted of regular firing (50%), bursting firing (33%), or irregular firing (17%). CCD also led to increased action potential duration which however was not normalized by $Na_V1.6$ or $Na_V\beta4$ knockdown. The cells with action potentials <1.5 msec were predominately cells with myelinated axons: in a subset of cells in which conduction velocity was measured, only 1 −2% of cells with action potentials <1.5 msec had conduction velocities in the C-fiber range, in any of the 4 experimental groups. Hence these cells had little effect on the reported summary data. Previous in vivo recordings of rat DRG neurons revealed a small percentage of cells with narrow action potentials and

C-fiber conduction velocities, that corresponded to low-threshold mechanoreceptors(Fang X et al., 2005), which may largely correspond to the 1–2% of cells we observed.

In cells with action potential durations >1.5 msec, (Figure 8), CCD led to a decrease in rheobase, however, the ameliorating effects of $Na_V1.6$ and $Na_V\beta4$ knockdown did not reach significance. AP duration was increased by CCD, but again there were no significant effects of $Na_V1.6$ or $Na_V\beta4$ knockdown. In general, most excitability parameters of cells with action potentials >1.5 msec were less affected by DRG compression, with only the decrease in rheobase and increase in percent cells firing multiple action potentials reaching significance. In these cells, none of the measured parameters differed significantly between the control siRNA-injected group and either the $Na_V1.6$ or $Na_V\beta4$ siRNA-injected groups, except that the lower level of spontaneous activity was significant for the $Na_V1.6$ knockdown group. The absolute levels of spontaneous activity were much less than that observed in cells with action potentials <1.5 msec. The cells with action potentials >1.5 msec were primarily C cells: In the subset of cells in which a conduction velocity could be measured, 96% of cells from normal DRG with action potentials >1.5 msec had C-fiber conduction velocities; this decreased to 75–81% in the 3 CCD groups. However, if the analysis was restricted to include only cells with a defined C-fiber conduction velocity, the conclusions presented above for cells with action potentials >1.5 msec were unchanged.

The CCD and LID models induce similar changes in pro- and anti-inflammatory cytokines that are little affected by $Na_V\beta4$ knockdown

Protein was isolated from inflamed or compressed DRGs 4 days after the pain model was implemented. siRNA (either control non-targeting or targeting $Na_V\beta4$) was injected just prior to implementing the pain model. A single sham operated group (involving similar exposure of the DRGs but without compression or inflammation) was used as the comparison group for both pain model groups, and data were expressed as the log of the fold increase from sham. Cytokines were measured using a multiplex method. Separate ANOVAs were run for the two pain models. The data are shown in Table 2, and some examples are plotted in figure 9.

The overall picture that emerged from the cytokine measurements was that the CCD and LID models had similar profiles, that were little affected by $Na_V\beta4$ knockdown. Most cytokines changed in the same direction for both models, though in some cases effects only reached significance in one of the models. This profile generally involved downregulation of anti-inflammatory or type 2 cytokines and upregulation of pro-inflammatory or type 1 cytokines. In Table 2, the cytokines have been divided into three groups. Group 1 consisted of cytokines that were significantly downregulated by either the CCD or LID model or both. This included several anti-inflammatory or Th2 cytokines such as IL-13 and IL-2, or cytokines induced by products of Th2 cells (eotaxin). IL-17 was also included in this group; this cytokine is generally considered pro-inflammatory but is related to a different subset of Th cells involved in type 1 inflammation. IL-12p70, a pro-inflammatory cytokine, was also downregulated. Group 2 consisted of cytokines that were significantly upregulated by CCD and/or LID. Many of these were pro-inflammatory, type 1 cytokines such as those involved in chemotaxis (MCP-1, MIP-1a) or associated with enhanced Th1 cell activity (e.g. IL-18,

IL-1β, IL-6). The third group consisted of cytokines not significantly regulated in either the LID or CCD groups.

Discussion

We found that knockdown of either $Na_V1.6$ or $Na_V\beta4$ reduced pain behaviors and sensory neuron hyperexcitability in the CCD model of low back pain. These findings are consistent with previous studies showing the importance of Na channels in mediating hyperexcitability and pain behaviors in this back pain model (see Introduction). We have now extended these findings by examining two specific Na channel isoforms. The observed effects of CCD on $Na_V1.6$ may account for previous reports showing a role for TTX-sensitive currents in mediating CCD-induced neuronal hyperexcitability. It is likely that additional currents are also affected by CCD, including TTX-resistant Na currents, K+ currents(Fan N,Donnelly DF and LaMotte RH, 2011) and hyperpolarization-activated cation currents(Song Y, Li HM, Xie RG, Yue ZF, Song XJ, Hu SJ and Xing JL, 2012). However, knock-down of either $Na_V1.6$ or $Na_V\beta4$ alone was sufficient to greatly ameliorate the effects of CCD on pain behaviors and neuronal excitability.

In other pain models we and others have observed that, as in this study, any manipulation that reduces abnormal spontaneous activity of sensory neurons improves pain behaviors(Devor M, 2009;Xie W, Strong JA, Kim D, Shahrestani S and Zhang JM, 2012;Xie W et al., 2009;Xie W, Strong JA and Zhang JM, 2015;Xie W, Tan ZY, Barbosa C, Strong JA, Cummins TR and Zhang J-M, 2016). In the CCD model, drugs that blocked spontaneous activity or targeted sodium channels while improving pain behaviors include thiamine,(Song XS, Huang ZJ and Song XJ, 2009) local bupivacaine nanoparticles,(Wang T et al., 2018) and lacosamide(Wang Y and Huo F, 2018). The spontaneous activity we observed was predominantly in cells with action potential durations <1.5 msec; these were likely predominantly cells with myelinated axons based on a subset of cells with measured conduction velocities. Similar results were previously reported for the CCD model(Hu SJ and Xing JL, 1998;Song XJ, Hu SJ, Greenquist KW, Zhang JM and LaMotte RH, 1999;Song Y, Li HM, Xie RG, Yue ZF, Song XJ, Hu SJ and Xing JL, 2012;Zhang J-M, Song XJ and LaMotte RH, 1999) and the LID model(Xie W, Strong JA, Kim D, Shahrestani S and Zhang JM, 2012). Knockdown of $Na_V\beta4$ can reduce spontaneous activity by reducing persistent and resurgent currents and by downregulating $Na_V1.6$(Buffington SA and Rasband MN, 2013;Cruz JS et al., 2011;Cummins TR et al., 2005;Lewis AH and Raman IM, 2014). We have previously shown that the $Na_V\beta4$ siRNA construct used in this study reduces resurgent currents and $Na_V1.6$ density in rat DRG neurons (Barbosa C et al., 2015;Xie W, Tan ZY, Barbosa C, Strong JA, Cummins TR and Zhang J-M, 2016). Examining the raw data made available by a study classifying mouse DRG sensory neurons into 11 subtypes according to their gene expression profiles(Usoskin D et al., 2015) shows that $Na_V1.6$ and $Na_V\beta4$ are extensively co-localized in all subtypes of cells with myelinated axons (72–100% of cells in each of the 6 myelinated subtypes express both isoforms) but not in any classes of unmyelinated cells (24% of tyrosine-hydroxylase expressing neurons and 0 to 14% of the other 4 unmyelinated subtypes show co-expression). The overall distribution profiles of $Na_V1.6$ and $Na_V\beta4$ observed in that study were similar to each other, and differed from the distribution of the $Na_V1.8$ channel that is commonly used as a marker of

nociceptors. Several mechanisms by which non-nociceptive, A-type neurons with myelinated axons might contribute to chronic pain states have been proposed(Devor M, 2009).

To our knowledge, specific Na channel isoforms have not been previously examined in the CCD model. However, $Na_V1.6$ has been implicated in other pain models, however, including neuropathic pain models(Henry MA et al., 2007;Xie W, Strong JA and Zhang JM, 2015), and chemotherapy induced pain(Sittl R et al.). $Na_V1.6$ knockdown in $Na_V1.8$-negative neurons was required to ameliorate pain in the spared nerve injury model of neuropathic pain(Chen L et al., 2018), consistent with previous studies implicating hyperexcitability of non-nociceptive neurons in $Na_V1.6$-dependent pathological pain. Oxaliplatin-induced cold allodynia relies on myelinated fibers in humans also(Forstenpointner J et al., 2018;Sittl R, Lampert A, Huth T, Schuy ET, Link AS, Fleckenstein J, Alzheimer C, Grafe P and Carr RW, 2012). A gain-of-function $Na_V1.6$ mutation in humans was recently proposed to exacerbate trigeminal neuralgia(Tanaka BS et al., 2016). Although $Na_V1.6$ is not considered to be a prime drug target for pain, due to its widespread distribution, targeting resurgent and persistent currents (or spontaneous activity) with peripherally restricted drugs might be a useful approach. These properties are more sensitive to certain channel blockers (such as some local anesthetics) than action potential propagation.

Overall the cytokine profile we observed in the CCD model (POD 4) was quite similar to that in the LID model as observed in this study (Table 2) and in 2 previous studies(Xie W, Chen S, Strong JA, Li AL, Lewkowich IP and Zhang J-M, 2016;Xie WR, Deng H, Li H, Bowen TL, Strong JA and Zhang J-M, 2006). The LID model involves a particular innate immunity stimulus (zymosan, a Toll-Like Receptor 2 agonist), but the CCD stimulus of tissue compression by the stainless steel rod also evoked elevation of type 1 pro-inflammatory cytokines and decrease of type 2 cytokines in our study. Hence the two models seem to share a similar overall immunological profile. Some of the same cytokines upregulated in our study have been implicated in human low back pain conditions(Kaufman EL and Carl A, 2013;Sutovsky J et al., 2017). The lack of effect of $Na_V\beta4$ knockdown on the cytokine profile in either model was unexpected, in light of previous studies suggesting multiple mechanisms for neurons to affect the cytokine profile by reciprocal interactions with non-neuronal cells. For example, neurons can be a source of cytokines (see Introduction), including cytokines that can attract or regulate macrophages and other immune cells(Foster SL et al., 2017;Kwon MJ et al., 2015;Verheijden S et al., 2015). Reducing neuronal activity reduces activation of satellite glia(Xie W, Strong JA and Zhang JM, 2009), another potential source of cytokines(Ji RR et al., 2016). However, our cytokine data suggest that, in both the LID and CCD models, sensory neuron activity is largely “downstream” of the cytokines studied. It will be of interest to look at other classes of inflammatory mediators to determine whether or not they are altered by reducing abnormal sensory neuron activity.

The CCD model was similar to the LID model in overall cytokine profile, and in the marked behavioral and electrophysiological effects of knocking down $Na_V1.6$ or $Na_V\beta4$. Some differences were observed, however: upregulation of $Na_V\beta4$ was observed only in the LID model (Xie W, Tan ZY, Barbosa C, Strong JA, Cummins TR and Zhang J-M, 2016), and the

degree of $Na_V1.6$ upregulation was smaller in the CCD model than in the LID model (Xie W, Strong JA, Ye L, Mao JX and Zhang J-M, 2013). The reduction in pain behaviors was more complete in the LID model after $Na_V1.6$ knockdown or $Na_V\beta4$ knockdown, than we observed here in the CCD model.

The reduction of pain behaviors by “microsympathectomy” (cutting the grey rami to L4 and L5) was robust, similar to that observed in the LID model(Xie W, Chen S, Strong JA, Li A-L, Lewkowich IP and Zhang J-M, 2016). Both CCD and LID models induce sympathetic sprouting in the DRG(Chien SQ et al., 2005;Xie WR, Deng H, Li H, Bowen TL, Strong JA and Zhang J-M, 2006). After CCD, sensory neurons may develop increased sensitivity to adrenergic and other sympathetic transmitters such as neuropeptide Y; conversely, blocking Na channels may have improved pain in part by reducing sympathetic sprouting (Wang Y and Huo F, 2018;Xie W et al., 2011;Zhang J-M et al., 2004). However, it is difficult to attribute all the behavioral effects of Na channel knockdown in our study to reduction of sympathetic sprouting into the DRG, as the behavioral effects were marked even on POD 1 while sympathetic sprouting develops more slowly(Chien SQ, Li C, Li H, Xie W, Pablo CS and Zhang JM, 2005). In the LID model, microsympathectomy has been show to also reduce local inflammation and inflammatory cytokine production(Xie W, Chen S, Strong JA, Li A-L, Lewkowich IP and Zhang J-M, 2016). These effects were more rapid, as needed to account for the effects of microsympathectomy on behavior observed in both models even at the earliest time points.

In summary, our study demonstrates that the $Na_V1.6$ and $Na_V\beta4$ subunits play largely similar roles in the CCD and LID models of low back pain. These two models also have similar cytokine profiles and sympathetic dependence. We suggest these models capture aspects of low back pain that are not dependent on the particular details of the model used and are broadly applicable to studying this condition. Although the broad tissue distribution of $Na_V1.6$ has made it a less appealing drug target, targeting abnormal spontaneous activity jointly facilitated by these two subunits may have therapeutic value.

Acknowledgements

This work was supported by in part by grants from the National Institute of Neurological Disorders and Stroke (NS045594, NS055860 to J-M Zhang), and National Institute of Arthritis and Musculoskeletal and Skin Diseases (AR068989 to J-M Zhang), Bethesda, MD, USA. The funding source had no role in any scientific aspects of the study. Declarations of interest: none.

List of abbreviations

DRG	dorsal root ganglia
LID	local inflammation of the DRG (back pain model)
CCD	chronic compression of the DRG (back pain model)
TTX	tetrodotoxin
mSYMPX	microsympathectomy (cutting grey rami to L4 and L5 DRG)
IL	interleukin

References

Barbosa C, Cummins TR (2016), Unusual Voltage-Gated Sodium Currents as Targets for Pain. Curr Top Membr 78:599–638. [PubMed: 27586296]

Barbosa C, Tan ZY, Wang R, Xie W, Strong JA, Patel RR, Vasko MR, Zhang J-M, et al. (2015), Navβ4 regulates fast resurgent sodium currents and excitability in sensory neurons. Molecular Pain 11:60. [PubMed: 26408173]

Baron R, Janig W, Kollmann W (1988), Sympathetic and afferent somata projecting in hindlimb nerves and the anatomical organization of the lumbar sympathetic nervous system of the rat. J Comp Neurol 275:460–468. [PubMed: 3225349]

Black JA, Renganathan M, Waxman SG (2002), Sodium channel Na(v)1.6 is expressed along nonmyelinated axons and it contributes to conduction. Brain Res Mol Brain Res 105:19–28. [PubMed: 12399104]

Buffington SA, Rasband MN (2013), Na+ channel-dependent recruitment of Navβ4 to axon initial segments and nodes of Ranvier. J Neurosci 33:6191–6202. [PubMed: 23554500]

Chaplan SR, Bach FW, Pogrel JW, Chung JM, Yaksh TL (1994), Quantitative assessment of tactile allodynia in the rat paw. Journal of Neuroscience Methods 53:55–63. [PubMed: 7990513]

Chen L, Huang J, Zhao P, Persson AK, Dib-Hajj FB, Cheng X, Tan A, Waxman SG, et al. (2018), Conditional knockout of NaV1.6 in adult mice ameliorates neuropathic pain. Sci Rep 8:3845. [PubMed: 29497094]

Chien SQ, Li C, Li H, Xie W, Pablo CS, Zhang JM (2005), Sympathetic Fiber Sprouting in Chronically Compressed Dorsal Root Ganglia Without Peripheral Axotomy. J Neuropathic Pain Symptom Palliation 1:19–23. [PubMed: 17387381]

Cruz JS, Silva DF, Ribeiro LA, Araujo IG, Magalhaes N, Medeiros A, Freitas C, Araujo IC, et al. (2011), Resurgent Na+ current: a new avenue to neuronal excitability control. Life Sci 89:564–569. [PubMed: 21683085]

Cummins TR, Dib-Hajj SD, Herzog RI, Waxman SG (2005), Nav1.6 channels generate resurgent sodium currents in spinal sensory neurons. FEBS Lett 579:2166–2170. [PubMed: 15811336]

Devor M (2009), Ectopic discharge in Aβ afferents as a source of neuropathic pain. Exp Brain Res 196:115–128. [PubMed: 19242687]

Dib-Hajj SD, Cummins TR, Black JA, Waxman SG (2010), Sodium channels in normal and pathological pain. Annu Rev Neurosci 33:325–347. [PubMed: 20367448]

Fan N, Donnelly DF, LaMotte RH (2011), Chronic compression of mouse dorsal root ganglion alters voltage-gated sodium and potassium currents in medium-sized dorsal root ganglion neurons. J Neurophysiol 106:3067–3072. [PubMed: 21917996]

Fan N, Sikand P, Donnelly DF, Ma C, Lamotte RH (2011), Increased Na+ and K+ currents in small mouse dorsal root ganglion neurons after ganglion compression. J Neurophysiol 106:211–218. [PubMed: 21525373]

Fang X, McMullan S, Lawson SN, Djouhri L (2005), Electrophysiological differences between nociceptive and non-nociceptive dorsal root ganglion neurones in the rat in vivo. J Physiol 565:927–943. [PubMed: 15831536]

Forstenpointner J, Oberlojer VC, Naleschinski D, Hoper J, Helfert SM, Binder A, Gierthmuhlen J, Baron R (2018), A-Fibers Mediate Cold Hyperalgesia in Patients with Oxaliplatin-Induced Neuropathy. Pain Pract 18:758–767. [PubMed: 29222932]

Foster SL, Seehus CR, Woolf CJ, Talbot S (2017), Sense and Immunity: Context-Dependent Neuro-Immune Interplay. Front Immunol 8:1463. [PubMed: 29163530]

Gu X, Wang S, Yang L, Sung B, Lim G, Mao J, Zeng Q, Chang Y, et al. (2007), Time-dependent effect of epidural steroid on pain behavior induced by chronic compression of dorsal root ganglion in rats. Brain Res 1174:39–46. [PubMed: 17869229]

Gu X, Wang S, Yang L, Sung B, Lim G, Mao J, Zeng Q, Yang CC, et al. (2007), A Rat model of radicular pain induced by chronic compression of lumbar dorsal root ganglion with Surgiflo. Anesthesiology 108:113–121.

Han WJ, Chen L, Wang HB, Liu XZ, Hu SJ, Sun XL, Luo C (2015), A Novel Nitronyl Nitroxide with Salicylic Acid Framework Attenuates Pain Hypersensitivity and Ectopic Neuronal Discharges in Radicular Low Back Pain. Neural Plast 2015:752782. [PubMed: 26609438]

Hasegawa Y, Mao W, Saha S, Gunner G, Kolpakova J, Martin GE, Futai K (2017), Luciferase shRNA Presents off-Target Effects on Voltage-Gated Ion Channels in Mouse Hippocampal Pyramidal Neurons. eNeuro 4.

Henry MA, Freking AR, Johnson LR, Levinson SR (2007), Sodium channel Nav1.6 accumulates at the site of infraorbital nerve injury. BMC Neurosci 8:56. [PubMed: 17662136]

Hu SJ, Xing JL (1998), An experimental model for chronic compression of dorsal root ganglion produced by intervertebral foramen stenosis in the rat. Pain 77:15–23. [PubMed: 9755014]

Huang ZJ, Hsu E, Li HC, Rosner AL, Rupert RL, Song XJ (2011), Topical application of compound Ibuprofen suppresses pain by inhibiting sensory neuron hyperexcitability and neuroinflammation in a rat model of intervertebral foramen inflammation. J Pain 12:141–152. [PubMed: 20797917]

Institute of Medicine (US) Committee on Advancing Pain Research C, and Education. (2011) Relieving Pain in America: A Blueprint for Transforming Prevention, Care, Education, and Research. Washington DC: National Academies Press.

Ji RR, Chamessian A, Zhang YQ (2016), Pain regulation by non-neuronal cells and inflammation. Science 354:572–577. [PubMed: 27811267]

Kaufman EL, Carl A (2013), Biochemistry of Back Pain. The Open Spine Journal 5:12–18.

Kwon MJ, Shin HY, Cui Y, Kim H, Thi AH, Choi JY, Kim EY, Hwang DH, et al. (2015), CCL2 Mediates Neuron-Macrophage Interactions to Drive Proregenerative Macrophage Activation Following Preconditioning Injury. J Neurosci 35:15934–15947. [PubMed: 26631474]

Lewis AH, Raman IM (2014), Resurgent current of voltage-gated Na(+) channels. J Physiol 592:4825–4838. [PubMed: 25172941]

Ma C, Greenquist KW, Lamotte RH (2006), Inflammatory mediators enhance the excitability of chronically compressed dorsal root ganglion neurons. J Neurophysiol 95:2098–2107. [PubMed: 16381809]

Ma ZL, Zhang W, Gu XP, Yang WS, Zeng YM (2007), Effects of intrathecal injection of prednisolone acetate on expression of NR2B subunit and nNOS in spinal cord of rats after chronic compression of dorsal root ganglia. Ann Clin Lab Sci 37:349–355. [PubMed: 18000292]

Nahm FS, Lee PB, Choe GY, Lim YJ, Kim YC (2017), Therapeutic effect of epidural hyaluronic acid in a rat model of foraminal stenosis. J Pain Res 10:241–248. [PubMed: 28182130]

Raman IM, Bean BP (1997), Resurgent sodium current and action potential formation in dissociated cerebellar Purkinje neurons. J Neurosci 17:4517–4526. [PubMed: 9169512]

Sittl R, Lampert A, Huth T, Schuy ET, Link AS, Fleckenstein J, Alzheimer C, Grafe P, et al. (2012), Anticancer drug oxaliplatin induces acute cooling-aggravated neuropathy via sodium channel subtype NaV1.6-resurgent and persistent current. Proc Natl Acad Sci U S A 109:6704–6709. [PubMed: 22493249]

Song XJ, Hu SJ, Greenquist KW, Zhang JM, LaMotte RH (1999), Mechanical and thermal hyperalgesia and ectopic neuronal discharge after chronic compression of dorsal root ganglia. J Neurophysiol 82:3347–3358. [PubMed: 10601466]

Song XS, Huang ZJ, Song XJ (2009), Thiamine suppresses thermal hyperalgesia, inhibits hyperexcitability, and lessens alterations of sodium currents in injured, dorsal root ganglion neurons in rats. Anesthesiology 110:387–400. [PubMed: 19194165]

Song Y, Li HM, Xie RG, Yue ZF, Song XJ, Hu SJ, Xing JL (2012), Evoked bursting in injured Abeta dorsal root ganglion neurons: a mechanism underlying tactile allodynia. Pain 153:657–665. [PubMed: 22237000]

Stebbing MJ, Eschenfelder S, Habler HJ, Acosta MC, Janig W, McLachlan EM (1999), Changes in the action potential in sensory neurones after peripheral axotomy in vivo. Neuroreport 10:201–206. [PubMed: 10203309]

Strong JA, Xie W, Bataille FJ, Zhang JM (2013), Preclinical studies of low back pain. Mol Pain 9:17. [PubMed: 23537369]

Sutovsky J, Benco M, Sutovska M, Kocmalova M, Pappova L, Miklusica J, Frano A, Kurca E (2017), Cytokine and chemokine profile changes in patients with lower segment lumbar degenerative spondylolisthesis. Int J Surg 43:163–170. [PubMed: 28600230]

Tan ZY, Donnelly DF, LaMotte RH (2006), Effects of a chronic compression of the dorsal root ganglion on voltage-gated Na+ and K+ currents in cutaneous afferent neurons. J Neurophysiol 95:1115–1123. [PubMed: 16424456]

Tanaka BS, Zhao P, Dib-Hajj FB, Morisset V, Tate S, Waxman SG, Dib-Hajj SD (2016), A gain-of-function mutation in Nav1.6 in a case of trigeminal neuralgia. Mol Med 22.

Usoskin D, Furlan A, Islam S, Abdo H, Lonnerberg P, Lou D, Hjerling-Leffler J, Haeggstrom J, et al. (2015), Unbiased classification of sensory neuron types by large-scale single-cell RNA sequencing. Nat Neurosci 18:145–153. [PubMed: 25420068]

Verheijden S, De Schepper S, Boeckxstaens GE (2015), Neuron-macrophage crosstalk in the intestine: a “microglia” perspective. Front Cell Neurosci 9:403. [PubMed: 26528133]

Wang T, Hurwitz O, Shimada SG, Tian D, Dai F, Zhou J, Ma C, LaMotte RH (2018), Anti-nociceptive effects of bupivacaine-encapsulated PLGA nanoparticles applied to the compressed dorsal root ganglion in mice. Neurosci Lett 668:154–158. [PubMed: 29355697]

Wang Y, Huo F (2018), Inhibition of sympathetic sprouting in CCD rats by lacosamide. Eur J Pain.

Watanabe K, Yabuki S, Sekiguchi M, Kikuchi S, Konno S (2011), Etanercept attenuates pain-related behavior following compression of the dorsal root ganglion in the rat. Eur Spine J 20:1877–1884. [PubMed: 21633793]

White FA, Sun J, Waters SM, Ma C, Ren D, Ripsch M, Steflik J, Cortright DN, et al. (2005), Excitatory monocyte chemoattractant protein-1 signaling is up-regulated in sensory neurons after chronic compression of the dorsal root ganglion. Proc Natl Acad Sci U S A 102:14092–14097. [PubMed: 16174730]

Xie W, Chen S, Strong JA, Li A-L, Lewkowich IP, Zhang J-M (2016), Localized sympathectomy reduces mechanical hypersensitivity by restoring normal immune homeostasis in rat models of inflammatory pain. J Neurosci 36:8712–8725. [PubMed: 27535916]

Xie W, Strong JA, Kays J, Nicol GD, Zhang JM (2012), Knockdown of the sphingosine-1-phosphate receptor S1PR1 reduces pain behaviors induced by local inflammation of the rat sensory ganglion. Neurosci Lett 515:61–65. [PubMed: 22445889]

Xie W, Strong JA, Kim D, Shahrestani S, Zhang JM (2012), Bursting activity in myelinated sensory neurons plays a key role in pain behavior induced by localized inflammation of the rat sensory ganglion. Neuroscience 206:212–223. [PubMed: 22265726]

Xie W, Strong JA, Mao J, Zhang JM (2011), Highly localized interactions between sensory neurons and sprouting sympathetic fibers observed in a transgenic tyrosine hydroxylase reporter mouse. Mol Pain 7:53. [PubMed: 21794129]

Xie W, Strong JA, Ye L, Mao JX, Zhang J-M (2013), Knockdown of sodium channel $Na_V1.6$ blocks mechanical pain and abnormal bursting activity of afferent neurons in inflamed sensory ganglia. Pain 154:1170–1180. [PubMed: 23622763]

Xie W, Strong JA, Zhang JM (2009), Early blockade of injured primary sensory afferents reduces glial cell activation in two rat neuropathic pain models. Neuroscience 160:847–857. [PubMed: 19303429]

Xie W, Strong JA, Zhang JM (2015), Local knockdown of the NaV1.6 sodium channel reduces pain behaviors, sensory neuron excitability, and sympathetic sprouting in rat models of neuropathic pain. Neuroscience 291:317–330. [PubMed: 25686526]

Xie W, Tan ZY, Barbosa C, Strong JA, Cummins TR, Zhang J-M (2016), Upregulation of the sodium channel NaVβ4 subunit and its contributions to mechanical hypersensitivity and neuronal hyperexcitability in a rat model of radicular pain induced by local DRG inflammation. Pain 157:879–891. [PubMed: 26785322]

Xie WR, Deng H, Li H, Bowen TL, Strong JA, Zhang J-M (2006), Robust increase of cutaneous sensitivity, cytokine production and sympathetic sprouting in rats with localized inflammatory irritation of the spinal ganglia. Neuroscience 142:809–822. [PubMed: 16887276]

Xu J, Brennan TJ (2010), Guarding pain and spontaneous activity of nociceptors after skin versus skin plus deep tissue incision. Anesthesiology 112:153–164. [PubMed: 19996955]

Yu Y, Huang X, Di Y, Qu L, Fan N (2017), Effect of CXCL12/CXCR4 signaling on neuropathic pain after chronic compression of dorsal root ganglion. Sci Rep 7:5707. [PubMed: 28720830]

Zhang H, Mei X, Zhang P, Ma C, White FA, Donnelly DF, Lamotte RH (2009), Altered functional properties of satellite glial cells in compressed spinal ganglia. Glia 57:1588–1599. [PubMed: 19330845]

Zhang J-M, Li H, Munir MA (2004), Decreasing sympathetic sprouting in pathologic sensory ganglia: a new mechanism for treating neuropathic pain using lidocaine. Pain 109:143–149. [PubMed: 15082136]

Zhang J-M, Song XJ, LaMotte RH (1997), An in vitro study of ectopic discharge generation and adrenergic sensitivity in the intact, nerve-injured rat dorsal root ganglion. Pain 72:51–57. [PubMed: 9272787]

Zhang J-M, Song XJ, LaMotte RH (1999), Enhanced excitability of sensory neurons in rats with cutaneous hyperalgesia produced by chronic compression of the dorsal root ganglion. Journal of Neurophysiology 82:3359–3366. [PubMed: 10601467]

Highlights

- Knock-down of sodium channel subunits $Na_V1.6$ and $Na_V\beta4$ reduced pain behaviors in the DRG compression model of low back pain
- The knock-down also reduced sensory neuron hyperexcitability and spontaneous activity, primarily in A-type neurons
- The 2 isoforms play similar roles in two low back pain models, DRG compression and DRG inflammation
- A similar pro-inflammatory cytokine profile is induced by both models, which was not affected by $Na_V\beta4$ knock-down
- Targeting the abnormal spontaneous activity mediated by $Na_V1.6$ and $Na_V\beta4$ may have therapeutic value

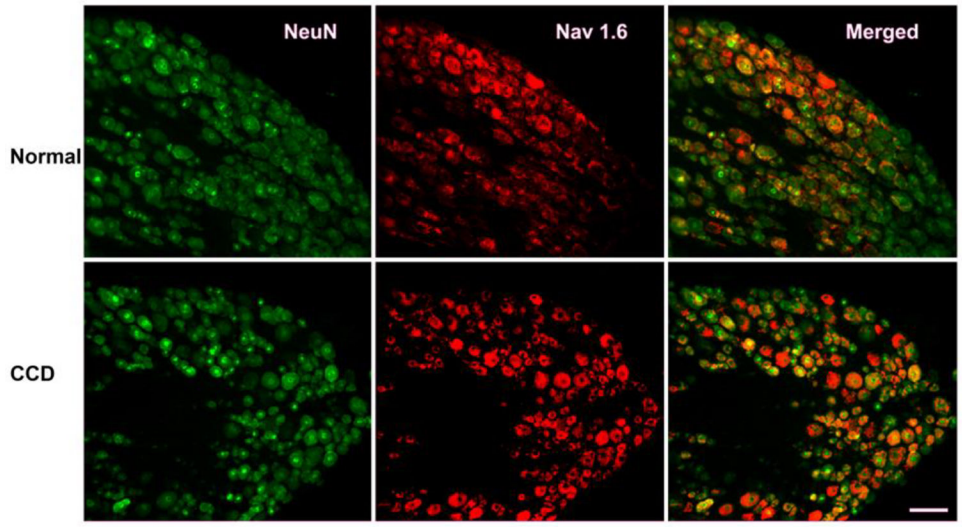

Figure 1.

Examples of $Na_V1.6$ immunostaining in normal and compressed DRGs. Sections from lumbar DRG were obtained from normal rats (top), or 4 days after DRG compression (bottom). Left: Green, NeuN labeling; Center: Red, $Na_V1.6$ (labeling); Right: merged images. Scale bar 100 μum.

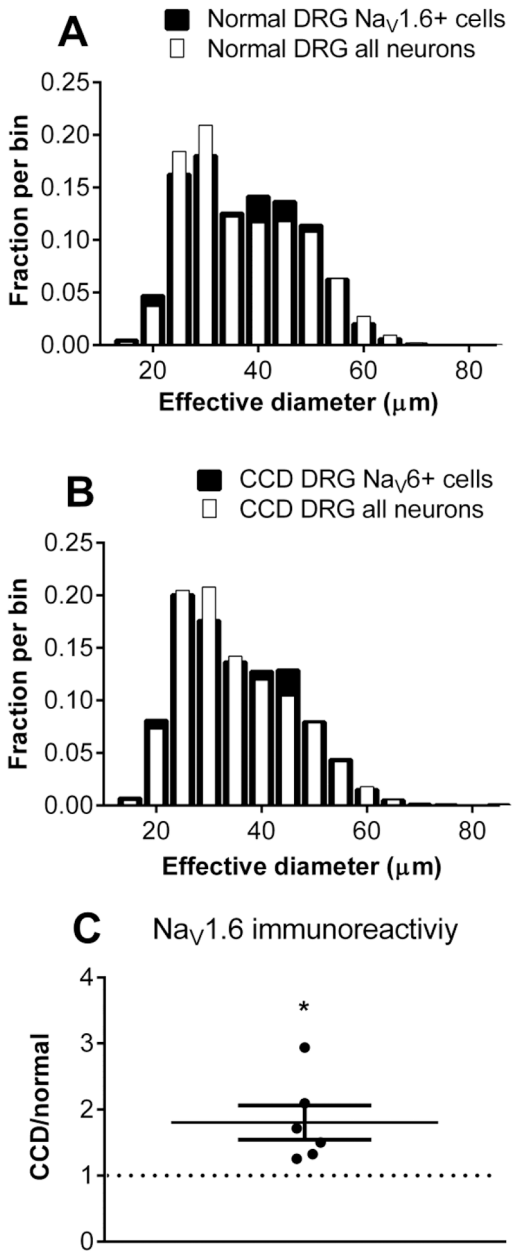

Figure 2.

Cell size distribution and overall intensity of $Na_V1.6$ immunostaining in normal and compressed DRGs. Areas of all neurons (NeuN-positive) and $Na_V1.6$-positive neurons were measured and expressed as the diameter of an equivalent circle. Distributions in normal DRG (A) and 4 days after CCD (B) are shown. N = 3 rats per group. C. Average intensity of Na 1.6 immunostaining increased after CCD. N = 6 L4 DRG and 6 L5 DRG/group (in separate experiments from A, B, without NeuN labelling). Intensity of $Na_V1.6$ in DRGs from CCD animals was normalized to that of normal animals measured in side-by-side experiments. *, $p<0.05$, significantly different from 1, one-sample t test.

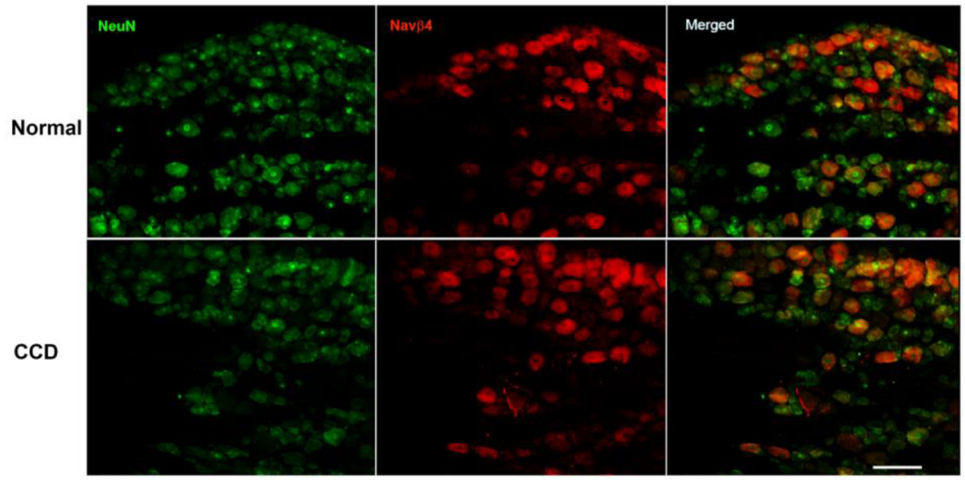

Figure 3.

Examples of $Na_V\beta4$ immunostaining in normal and compressed DRGs. Sections from lumbar DRG were obtained from normal rats (top), or 4 days after DRG compression (bottom). Left: Green, NeuN labeling; Center: Red, $Na_V\beta4$ labeling; Right: merged images. Scale bar 100 μm.

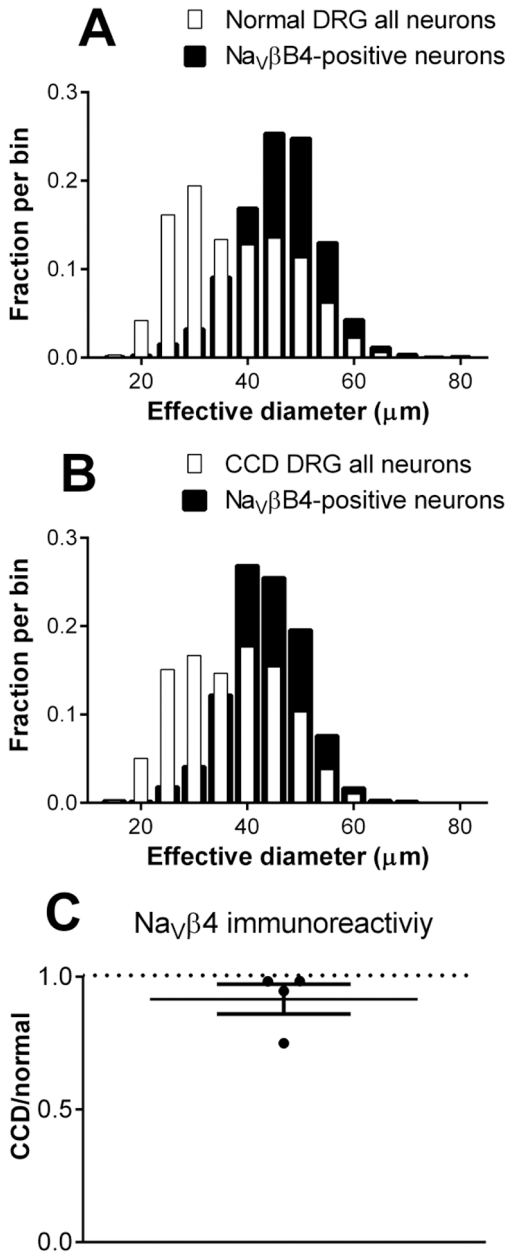

Figure 4.

Cell size distribution and overall intensity of $Na_V\beta4$ immunostaining in normal and compressed DRGs. Areas of all neurons (NeuN-positive) and $Na_V1.6$-positive neurons were measured and expressed as the diameter of an equivalent circle. Distributions in normal DRG (A) and 4 days after CCD (B) are shown. N = 5 rats per group. C. Average intensity of $Na_V\beta4$ immunostaining increased after CCD. N =4 rats/group (in separate experiments from A, B). Intensity of $Na_V\beta4$ in DRGs from CCD animals was normalized to that of normal animals measured in side-by-side experiments. Average ratio did not differ significantly different from 1, one-sample t test, p = 0.23.

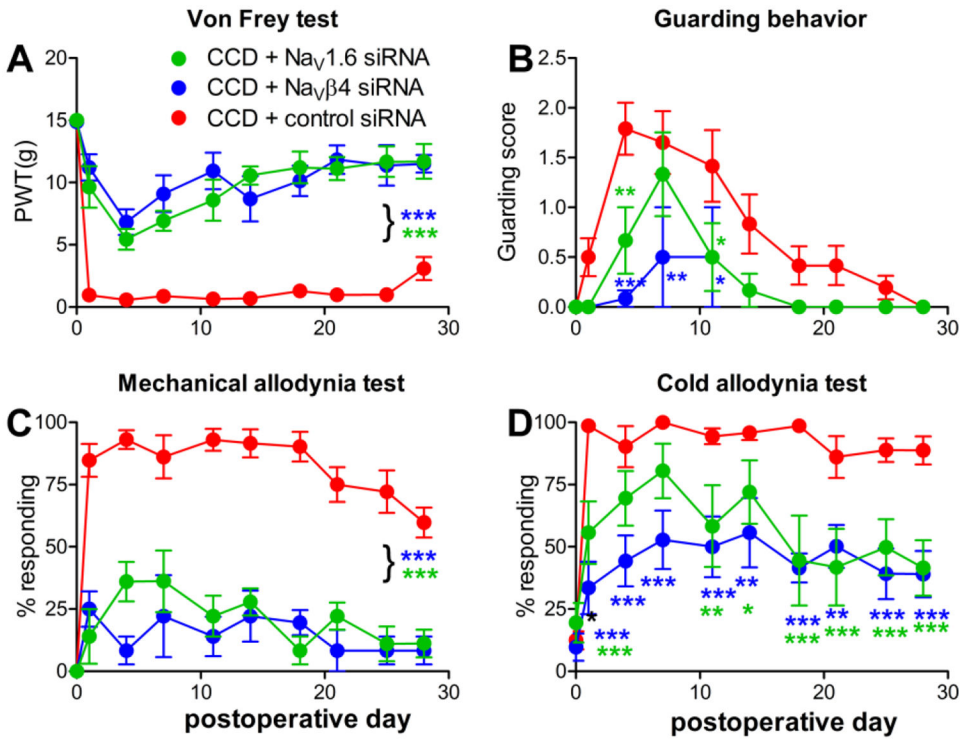

Figure 5.

Knockdown of $Na_V1.6$ or $Na_V\beta4$ reduces pain behaviors in the chronic compression of the DRG (CCD) model. siRNA directed against the indicated sodium channel isoform, or non-targeting control siRNA, was injected into the L4 and L5 DRG just prior to compression. Baseline (average of 2 measurements) is plotted on day 0. A, static mechanical threshold (von Frey test). B. Guarding score (spontaneous pain). C. Dynamic mechanical allodynia (cotton wisp test). D. Cold allodynia (acetone test). *, $p<0.05$; **, $p<0.01$, ***, $p<0.001$; significant difference between the $Na_V1.6$ (green symbols) or $Na_V\beta4$ (blue symbols) group and the control siRNA group at the indicated time points or (with bracket) at all post-baseline time points (two-way repeated measures ANOVA with Holm-Sidak posttest comparing each group with the control group). Data shown combine two separate experiments in which either $Na_V1.6$ or $Na_V\beta4$ knockdown animals were compared with control knockdown animals in side-by-side measurements. Control data looked very similar in both groups and have been combined for the plot and for statistical analysis. N = 6 animals/group ($Na_V1.6$; $Na_V\beta4$) or 12 animals group (2 combined control groups). Overall p values and $F_{(2,21)}$ for the group factor in the ANOVA analysis were: A, $p<0.0001$, $F=96.14$; B, $p= 0.0056$, $F=6.702$; C, $p<0.0001$, $F = 73.55$; D, $p<0.0001$. $F= 21.68$.

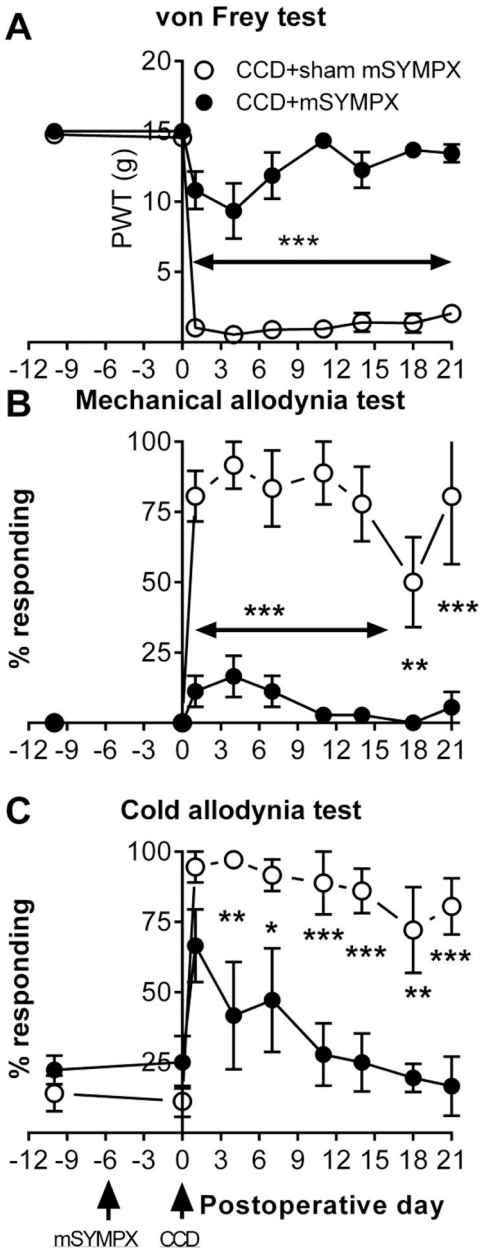

Figure 6.

Prior "microsympathectomy" reduces pain behaviors induced by DRG compression. Two baseline measurements were obtained, their average is plotted on day −10. Microsympathectomy (cutting of the grey rami to the L4 and L5 DRG; "mSYMPX") or sham mSYMPX was performed on day −6. Baselines were measured again on day 0, just prior to chronic compression of the DRG ("CCD"). A, static mechanical threshold (von Frey test). B. Dynamic mechanical allodynia (cotton wisp test). C. Cold allodynia (acetone test). *, $p<0.05$; **, $p<0.01$, ***, $p<0.001$; significant difference between the sham and mSYMPX groups at the indicated time points (two-way repeated measures ANOVA with Holm-Sidak posttest). N = 6 male rats per group. Overall p values and $F_{(1,10)}$ for the group factor were: A, $p<0.001$, $F=129.9$; B, $p<0.0001$, $F=49.13$; C, $p=0.0024$, $F=16.28$.

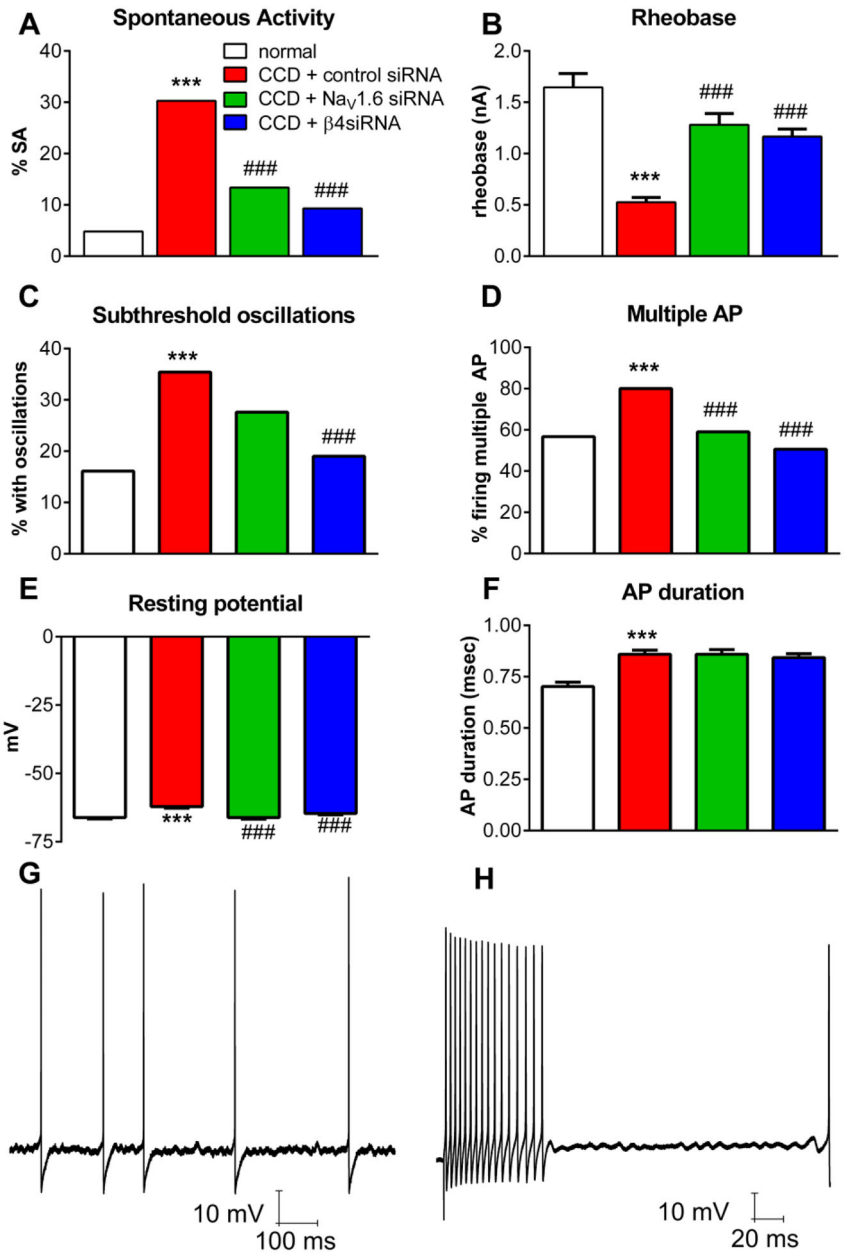

Figure 7.

Knockdown of $Na_V1.6$ or $Na_V\beta4$ reduces hyperexcitability of DRG neurons with narrow action potentials induced by chronic compression of the DRG (CCD). siRNA directed against the indicated sodium channel isoform, or non-targeting control siRNA, was injected into the L4 and L5 DRG just prior to compression, and DRGs were isolated 4 days later for microelectrode recording in a whole DRG preparation. Normal DRG were obtained from unoperated animals of the same age. Data are from all cells with action potential duration <1.5 msec. A, incidence of spontaneous activity. B, rheobase (defined as zero for spontaneously active cells). C. Percentage of cells in which subthreshold membrane potential oscillations were observed during spontaneous activity or during current injection. D. Percentage of cells capable of firing more than 2 action potentials during 270 msec

depolarizing current injections. E, resting membrane potential. F. Duration of the action potential, measured at threshold. Examples of recordings of membrane oscillations (as tabulated in C) are shown from a spontaneously active cell (G), and a cell in which oscillations were evoked in response to suprathreshold current injection (H); both cells are from the CCD + non-targeting siRNA group. *, $p<0.05$; **, $p<0.01$, ***, $p<0.001$; significant difference between the control and CCD (control siRNA) groups; #, $p<0.05$; ##, $p<0.01$, ###, $p<0.001$; significant difference between the CCD (control siRNA) group and the $Na_V1.6$ or $Na_V\beta4$ groups, based on Kruskal-Wallis test with Dunn's posttest (continuous variables) or chi-square test (variables with percentage). N = 104 (normal) from 3 rats, 165 (CCD + control siRNA) from 3 rats, 134 (CCD + $Na_V1.6$ siRNA) from 4 rats, and 172 (CCD + $Na_V\beta4$ siRNA) from 6 rats. Rats were of similar weight and size as rats used in the behavior experiments shown in Figure 5.

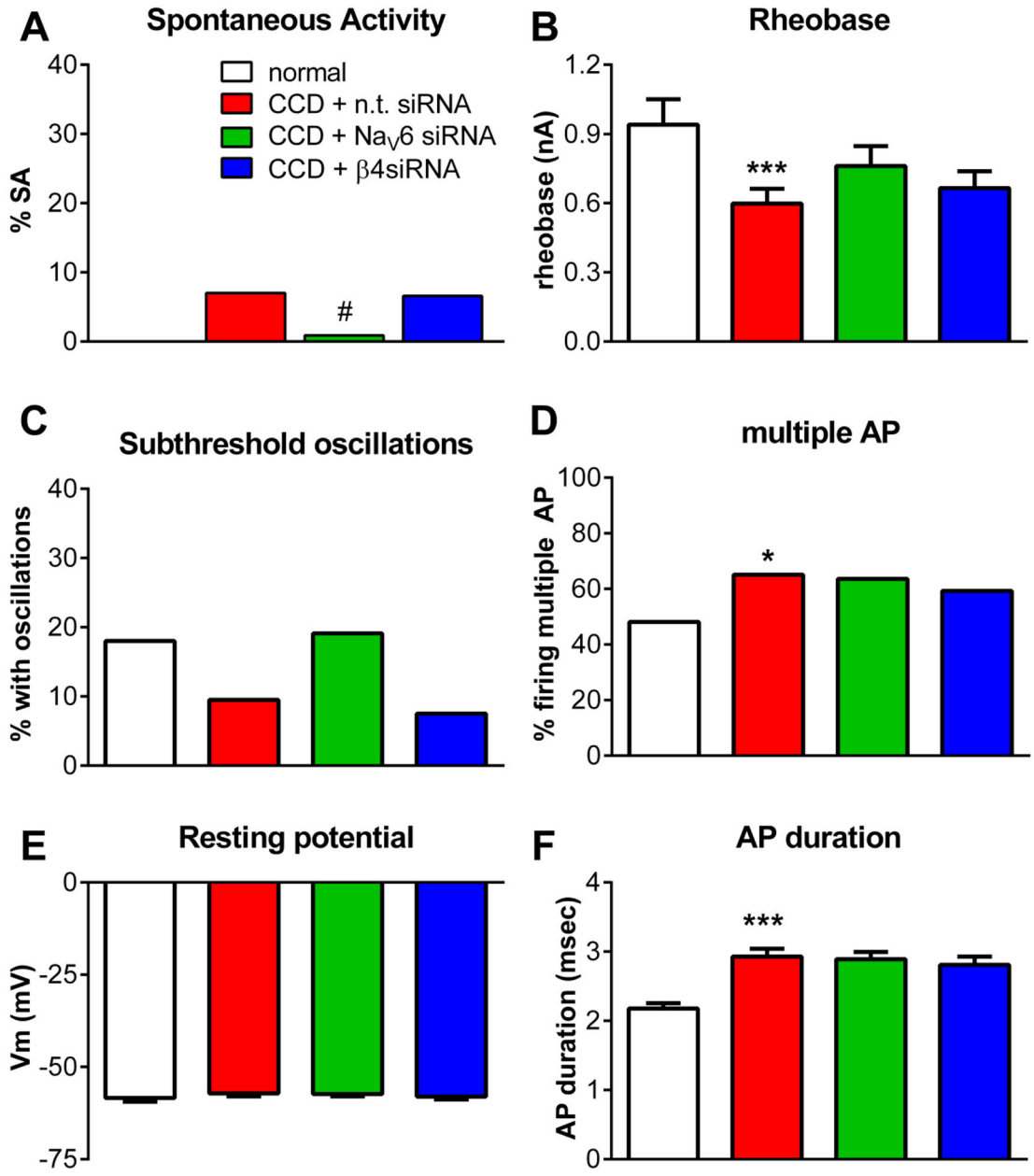

Figure 8.

Effects of knockdown of $Na_V1.6$ or $Na_V\beta4$ on excitability of DRG neurons with action potential durations >1.5 msec after chronic compression of the DRG (CCD). siRNA directed against the indicated sodium channel isoform, or non-targeting control siRNA, was injected into the L4 and L5 DRG just prior to compression, and DRGs were isolated 4 days later for microelectrode recording in a whole DRG preparation. Normal DRG were obtained from unoperated animals of the same age. Data are from all cells with action potential duration >1.5 msec. A, incidence of spontaneous activity (value is zero for normal DRG). B, rheobase. C. Percentage of cells in which subthreshold membrane potential oscillations were observed during spontaneous activity or during current injection. D. Percentage of cells capable of firing more than 2 action potentials during 270 msec depolarizing current

injections. E, resting membrane potential. F. Duration of the action potential, measured at threshold. ***, $p<0.001$; significant difference between the control and CCD (control siRNA) groups; #, $p<0.05$, significantly different from CCD (control siRNA) groups. Comparisons were made using Kruskal-Wallis test with Dunn's posttest (continuous variables) or chi-square test (variables with percentage). N = 52 (normal), 86 (CCD + control siRNA), 107 (CCD + $Na_V1.6$ siRNA), and 91 (CCD + $Na_V\beta4$ siRNA). Rats (same rats as Figure 7) were of similar weight and size as rats used in the behavior experiments shown in Figure 5.

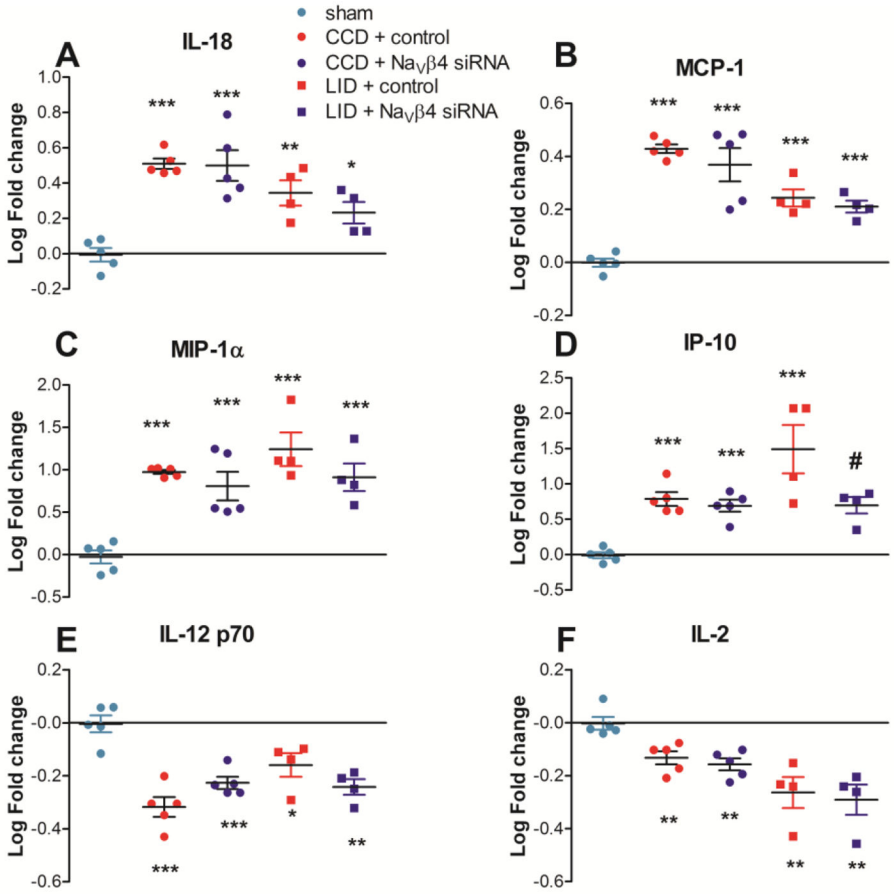

Figure 9.

Effect of compression or inflammation of the DRG on DRG cytokine levels. Non-targeting control siRNA (red) or siRNA directed against $Na_V\beta4$ (blue) was injected at the time of DRG compression ("CCD", solid bars) or local DRG inflammation ("LID", hatched bars). Cytokine levels were normalized to that of the sham operated group and log-transformed. A – D, examples of pro-inflammatory cytokines increased by LID and CCD. E – F, examples of anti-inflammatory cytokines downregulated by LID and CCD. *, $p<0.05$; **, $p<0.01$; ***, $p<0.001$, significantly different from sham group; #, $p<0.05$ significantly different from LID + n.t. siRNA group (ANOVAs with Tukey's posttest comparing the sham, CCD + control, and CCD + $Na_V\beta4$ siRNA groups or comparing the sham, LID + control, and LID + $Na_V\beta4$ groups). N = 4 – 5 rats per group (see also Table 2).

Table 1.

Full, systemic and alternative names of cytokines examined

Name in text	Full Name	Alternative and Systemic Names
EGF	Epidermal Growth Factor	
Eotaxin	Eotaxin	CCL11
Fractalkine	Fractalkine	CX3CL1
IL-12p70	Interleukin-12	p70 refers to the active heterodimer
IL-13	Interleukin-13	
IL-17A	Interleukin-17A	CTLA-8
IL-18	Interleukin-18	Interferon-gamma inducing factor
IL-1α	Interleukin-1α	
IL-1β	Interleukin-1β	
IL-2	Interleukin-2	
IL-4	Interleukin-4	
IL-6	Interleukin-6	
IP-10	Interferon γ-induced Protein 10	CXCL10
Leptin	Leptin	Ob gene
MCP-1	Monocyte chemotactic protein 1	CCL2
MIP-1α	Macrophage inflammatory Protein 1α	CCL3
MIP-2	Macrophage inflammatory protein 2	CXCL2
RANTES	Regulated on activation, normal T cell expressed and secreted	CCL5
TNFα	Tumor necrosis factor α	
VEGF	Vascular endothelial growth factor	

Table 2.

Effect of back pain models and $Na_V\beta4$ knockdown on DRG cytokines CCD, chronic compression of the DRG (day 4). LID, local inflammation of the DRG (Day 4). n.t., non-targeting siRNA.

		SHAM (n = 5)		CCD + n.t. siRNA (n = 5) Avg. log fold change ± SEM	CCD + β4 siRNA (n = 5)		LID + n.t. siRNA (n = 4)		LID + βB4 siRNA (n = 4)	
	Cytokine	Avg. log fold change ± SEM	Fold increase[a]		Fold increase	Avg. log fold change ± SEM	Fold increase	Avg. log fold change ± SEM	Fold increase	Avg. log fold change ± SEM
Group 1	EGF	−0.02 ± 0.07	0.46	−0.34 ± 0.10	0.77	−0.11 ± 0.23	0.16	−0.80 ± 0.12**	0.19	−0.73 ± 0.19**
	IL-12p70	0.00 ± 0.03	0.48	−0.32 ± 0.04***	0.59	−0.23 ± 0.02***	0.69	−0.16 ± 0.04*	0.57	−0.24 ± 0.03**
	IL-13	−0.01 ± 0.04	0.70	−0.15 ± 0.01**	0.74	−0.13 ± 0.02*	0.62	−0.21 ± 0.05	0.61	−0.21 ± 0.09
	IL-2	0.00 ± 0.02	0.74	−0.13 ± 0.02**	0.70	−0.16 ± 0.02**	0.54	−0.26 ± 0.06**	0.51	−0.29 ± 0.06**
	Eotaxin	0.00 ± 0.03	0.81	−0.09 ± 0.02*	0.87	−0.06 ± 0.01	0.69	−0.16 ± 0.06	0.67	−0.18 ± 0.06
	IL-17A	0.00 ± 0.02	0.74	−0.13 ± 0.02**	0.75	−0.12 ± 0.02**	0.78	−0.11 ± 0.02	0.56	0.25 ± 0.04***#
Group 2	RANTES	−0.01 ± 0.04	1.47	0.17 ± 0.08	1.12	0.05 ± 0.11	2.20	0.34 ± 0.02***	2.43	0.39 ± 0.06***
	IL-1β	−0.01 ± 0.05	1.95	0.29 ± 0.04	2.06	0.31 ± 0.13*	10.65	1.03 ± 0.20**	5.15	0.71 ± 0.20*
	MCP-1	0.00 ± 0.02	2.68	0.43 ± 0.02***	2.34	0.37 ± 0.06***	1.75	0.24 ± 0.03***	1.62	0.21 ± 0.02***
	IL-6	0.00 ± 0.03	3.19	0.50 ± 0.04***	2.42	0.38 ± 0.08***	1.22	0.08 ± 0.04	1.02	0.01 ± 0.02
	IL-18	−0.01 ± 0.04	3.23	0.51 ± 0.03***	3.16	0.50 ± 0.09***	2.21	0.34 ± 0.07**	1.71	0.23 ± 0.06*
	IP-10	−0.01 ± 0.04	6.14	0.79 ± 0.10***	4.92	0.69 ± 0.08***	31.08	1.49 ± 0.34***	4.98	0.70 ± 0.12#
	MIP-1α	−0.03 ± 0.08	9.42	0.97 ± 0.02***	6.42	0.81 ± 0.17***	17.48	1.24 ± 0.20***	8.17	0.91 ± 0.16**
Group 3	IL-4	−0.01 ± 0.03	0.90	−0.04 ± 0.03	0.80	−0.10 ± 0.03	0.82	−0.08 ± 0.03	0.72	−0.14 ± 0.03*
	Leptin	−0.02 ± 0.07	0.96	−0.02 ± 0.06	0.96	−0.02 ± 0.11	0.68	−0.17 ± 0.03	0.47	−0.33 ± 0.06**
	TNFα	0.00 ± 0.03	1.00	0.00 ± 0.02	1.03	0.01 ± 0.02	1.07	0.03 ± 0.02	1.06	0.03 ± 0.01
	VEGF	0.00 ± 0.02	1.01	0.00 ± 0.03	0.88	−0.05 ± 0.02	0.86	−0.07 ± 0.02	0.70	−0.15 ± 0.05*
	MIP-2	0.00 ± 0.02	1.03	0.01 ± 0.04	0.84	−0.07 ± 0.03	1.12	0.05 ± 0.13	0.69	−0.16 ± 0.07
	IL-1α	−0.02 ± 0.07	1.26	0.10 ± 0.03	1.27	0.10 ± 0.07	1.71	0.23 ± 0.14	0.91	−0.04 ± 0.19
	Fractalkine	−0.01 ± 0.03	1.27	0.10 ± 0.03	1.35	0.13 ± 0.08	1.12	0.05 ± 0.01	0.90	−0.04 ± 0.04

CCD, chronic compression of the DRG (day 4). LID, local inflammation of the DRG (Day 4). n.t., non-targeting siRNA.

*, $p < 0.05$;

** , $p < 0.01$;

*** , $p < 0.001$, significantly different from sham group.

, $p < 0.05$ significantly different from LID + n.t. siRNA group.

[a] Anti-log of log fold change is shown for ease of reading. Statistics were applied to log-transformed data.